Oxidation of Cytochrome *c* by Cytochrome *c* Oxidase: Spectroscopic Binding Studies and Steady-State Kinetics Support a Conformational Transition Mechanism†

Bruno Michel and Hans Rudolf Bosshard*

Biochemisches Institut der Universität Zürich, Winterthurerstrasse 190, CH-8057 Zürich, Switzerland

Received March 22, 1988; Revised Manuscript Received June 13, 1988

ABSTRACT: The long-known biphasic response of cytochrome *c* oxidase to the concentration of cytochrome *c* has been explained, alternatively, by the presence of a catalytic and a regulatory site on the oxidase, by negative cooperativity between adjacent active sites in dimeric oxidase, or by a transition of the enzyme molecule between different conformational states. The three mechanistic hypotheses allow testable predictions about the relationship between substrate binding and steady-state kinetics catalyzed by the monomeric and dimeric (or oligomeric) enzyme. We have tested these predictions on monomeric, dimeric, and oligomeric beef heart oxidase and on monomeric oxidase from *Paracoccus denitrificans*. The aggregation state of the oxidase was evaluated from the sedimentation equilibrium in the ultracentrifuge and by gel chromatography. The binding of cytochrome *c* to cytochrome *c* oxidase was measured by spectrophotometric titration of cytochrome *c* oxidase with cytochrome *c*. The procedure makes use of a small perturbation in the Soret band of the absorption spectrum of the cytochrome *c*–cytochrome *c* oxidase complex. The steady-state oxidation of cytochrome *c* was followed spectroscopically by an automated assay procedure, and the kinetic parameters were deduced by numerical analysis of several hundred initial rate assays in the substrate concentration range 0.15–30 μM. The following results were obtained: (1) The kinetics of cytochrome *c* oxidation are always biphasic at low ionic strength, independent of the aggregation state of the enzyme. (2) The kinetics become apparently monophasic at ionic strengths above 100 mM or at slightly acidic pH values. (3) Binding of cytochrome *c* to cytochrome *c* oxidase is always monophasic and is always to a single binding site per heme aa_3, independent of the aggregation state of the enzyme. These results are compatible with a conformational transition mechanism; they are not compatible with either negative cooperativity or regulatory site models. A minimal scheme for a transition mechanism accounting for the observed pH and ionic strength dependence of cytochrome *c* oxidation is presented. In the proposed mechanism the enzyme oscillates between two conformational states, one of high affinity and the other of low affinity for cytochrome *c*. The transition is strongly coupled to the electron-transfer process.

The rate of oxidation of cytochrome *c* catalyzed by cytochrome *c* oxidase, which is the final enzyme of the mitochondrial respiratory chain, does not obey Michaelis–Menten kinetics. The kinetic behavior has been called nonlinear, referring to the graphical presentation methods for kinetic data, for example, the widely used Eadie–Hofstee plot. The kinetic features of cytochrome *c* oxidase have intrigued enzymologists ever since the pioneering studies of Keilin (1930) [review by Nicholls (1974)]. Different mechanisms were proposed to explain the nonlinearity of the reaction (Smith & Conrad, 1956; Minnaert, 1961; Nicholls, 1965; Nicholls & Chance, 1974; Errede et al., 1976; Ferguson-Miller et al., 1976, 1978; Capaldi et al., 1982; Antalis & Palmer, 1982; Wainio, 1983; Nalecz et al., 1983; Brzezinski & Malmström, 1986), but the molecular interpretation of the oxidase kinetics is still controversial (Speck et al., 1984; Bolli et al., 1985; Sinjorgo et al., 1986; Brzezinski & Malmström, 1986; Brzezinski et al., 1986).

The nonlinearity is thought to be inherent in the complexity of the reaction (Antalis & Palmer, 1982): transfer of four electrons from the single-electron donor cytochrome *c* to the four-electron acceptor oxygen and coupling of this exergonic process to the endergonic translocation of protons across the inner mitochondrial membrane. This is achieved by a set of four redox centers embedded in a membrane-spanning enzyme composed of 13 different polypeptide chains (Wikström et al., 1981). The redox centers consist of two spectroscopically distinguishable hemes, hemes *a* and a_3, and of two, or possibly three (Steffens et al., 1987), copper ions. In its isolated form, mitochondrial oxidase can exist in different aggregation states, oligomeric, dimeric, and monomeric, depending on the isolation procedure and the detergent used for protein dispersion[1] (Georgevich et al., 1983; Suarez et al., 1984; Sinjorgo et al., 1986; Robinson & Talbert 1986; Nalecz et al., 1986). The aggregation state of the enzyme in the inner mitochondrial membrane is not known. Bacterial oxidases are of much simpler subunit composition and are mostly monomeric (Ludwig & Schatz, 1979; Ludwig, 1980; Ludwig et al., 1982; Poole, 1983).

Three different mechanisms are currently discussed to explain the nonlinear overall reaction with reduced cytochrome *c*. There are variants to each of the three mechanisms.

† Supported in part by the Swiss National Science Foundation (Grant 3.114.85), the Hartmann-Müller Stiftung, and the Kanton of Zürich.

* To whom correspondence should be addressed.

[1] Independent of the aggregation state, the concentration of the oxidase is always expressed as the concentration of the sum of heme $a + a_3$, referred to as heme aa_3. Dimeric enzyme contains two heme aa_3 "units" and, in the case of the enzyme from beef heart, has a nominal molecular mass of about 400 kDa deduced from the sequence of the 13 different polypeptide chains (Buse et al., 1985).

0006-2960/89/0428-0244$01.50/0

The *regulatory site mechanism* envisages a single catalytic site per heme aa_3 (Speck et al., 1984; Sinjorgo et al., 1984, 1986). Adjacent to the catalytic site is at least one regulatory site where cytochrome *c* binds without transferring electrons. Cytochrome *c* bound to the regulatory site weakens binding of cytochrome *c* at the catalytic site, thereby reducing the affinity of the enzyme for both substrate and product. The model explains both the appearance of a low-affinity/high-velocity second phase at high substrate concentration and the ionic strength dependence of the overall reaction, provided that product dissociation is rate limiting.

In the *negative cooperativity mechanism* there is also a single catalytic site per heme aa_3 (Capaldi et al., 1982; Nalecz et al., 1983). In the dimeric enzyme two catalytic sites are brought close together in such a way that occupation of one site by cytochrome *c* interferes with binding of cytochrome *c* to the adjacent catalytic site because of electrostatic repulsion between the strongly basic cytochrome *c* molecules and/or by steric repulsion. In contrast to the regulatory site mechanism, the nonlinearity is now the exclusive property of dimeric and oligomeric oxidase. The model is based on the topographical features of beef heart oxidase obtained by electron microscopy and image reconstruction (Fuller et al., 1979) and on the results from chemical cross-linking of cytochrome *c* to oxidase (Darley-Usmar et al., 1983).

In the *conformational transition mechanism* the enzyme oscillates between two different conformations, one of high affinity and the other of low affinity for cytochrome *c* (Malmström, 1985; Brzezinski & Malmström, 1986). The transition between the conformations is strongly coupled to the electron-transfer process. The two conformations are compulsory intermediates of the vectorial proton translocation.[2]

Common to the three mechanisms is a single catalytic site for electron transfer by reduced cytochrome *c*. There is indeed strong and manyfold evidence for a single catalytic site per heme aa_3 (Michel & Bosshard, 1984; Speck et al., 1984; Sinjorgo et al., 1986).

The three mechanisms make unique and testable predictions about the nature of the binding of cytochrome *c* to the oxidase and about the steady-state kinetics of cytochrome *c* oxidation. In the negative cooperativity mechanism biphasic kinetics would only be observed with dimeric and oligomeric oxidase. Binding of cytochrome *c* to the monomeric oxidase would be linear, and nonlinear to the dimeric and oligomeric oxidase. (Here, linear and nonlinear refer to the usual Scatchard representation of binding data.) The regulatory site mechanism is characterized by nonlinear oxidation kinetics and nonlinear cytochrome *c* binding, independent of the aggregation state of the enzyme. In the conformational transition mechanism cytochrome *c* oxidation would also be nonlinear for all of the aggregation states of the enzyme. Binding of cytochrome *c* to the resting oxidase would in this case be linear since the enzyme cannot exist in different conformations except when transferring electrons.

We have tested these predictions by independently measuring both the binding of cytochrome *c* and the kinetics of cytochrome *c* oxidation, using oligomeric, dimeric, and monomeric beef heart oxidase and monomeric bacterial oxidase from *Paracoccus denitrificans*. An extensive series of experiments were performed at different ionic strength and pH values and with the enzyme dispersed in different detergents. Binding of cytochrome *c* to the oxidase was followed by a spectrophotometric titration method (Michel & Bosshard, 1984). For the steady-state kinetic assays a computer-controlled mixing robot and data handling system was used (Michel, 1988a,b). With this novel device the kinetic parameters could be deduced from large sets of highly reproducible primary data.

We find that binding of cytochrome *c* to cytochrome *c* oxidase is always of the linear type, whether the enzyme is monomeric, dimeric, or oligomeric. In contrast, the oxidation of cytochrome *c* always follows a biphasic pattern at low ionic strength and neutral pH, independent of the aggregation state of the enzyme. The results support the conformational transition mechanism. A minimal model is proposed to qualitatively explain the pH and ionic strength dependence of cytochrome *c* oxidation.

Experimental Procedures

Materials. Beef heart oxidase was prepared according to the method of Hartzell and Beinert (1974). The last pellet of the ammonium sulfate fractionation was homogenized in a minimal volume of 10 mM Tris-HCl, pH 7.4, and 15 mM NaCl and stored at −80 °C. All experiments were performed on the same batch of enzyme obtained from four beef hearts.

To exchange the detergent, the last pellet from the ammonium sulfate precipitate was diluted 30 times in 10 mM Tris-HCl, pH 7.4, containing the detergent of choice and applied to a column (1.5 × 9 cm) of DE-32 cellulose (Whatman). The column was washed with 10 volumes of the above Tris buffer and the oxidase eluted with the same buffer containing 200 mM NaCl. The enzyme was concentrated by ultrafiltration (Amicon membrane UF C100) to a concentration of about 120 μM in 10 mM Tris-HCl, pH 7.4, 15 mM NaCl, and detergent (0.1% lauryl maltoside or 0.2% Tween 80). For binding experiments and kinetic assays, the enzyme was diluted from this stock solution and brought to the desired ionic strength by adding NaCl.

Monomeric beef heart oxidase was prepared according to the method of Georgevich et al. (1983). Briefly, the last homogenate from the ammonium sulfate precipitation was incubated with an equal volume of 0.64 M Tris-HCl, pH 8.5, and 10% Triton X-100 for 2 h on ice. The sample was diluted 30 times by distilled water and applied to the DE-32 ion-exchange column for detergent exchange, as described above.

The beef heart oxidase had a heme content of 9 nmol of heme *a*/mg of protein (determined by the Coomassie blue method, using bovine serum albumin as a standard; Bradford, 1976). The ratio $\epsilon_{444}^{red}/\epsilon_{422}^{ox}$ was 1.37 and $\epsilon_{280}/\epsilon_{420}^{ox}$ was 2.5. The lipid phosphorus content was 18 ± 1 mol/mol of heme aa_3 [determined according to the method of Chen et al. (1956)]. The concentration of heme aa_3 was calculated with the extinction coefficients given by van Gelder (1966).

For partial proteolysis, beef cytochrome *c* oxidase (50 μM) was treated with α-chymotrypsin (Fluka, Buchs, Switzerland) in 50 mM sodium phosphate buffer, pH 7.8, and 0.5% cholate for 3 h at 20 °C. The chymotrypsin to oxidase ratio was 1/20 (w/w). Proteolytic fragments and chymotrypsin were separated from the partially digested oxidase on a column of Sepharose AcA 54 (Pharmacia), equilibrated and eluted with 10 mM Tris-HCl, pH 7.4, 15 mM NaCl, and 0.2% Tween 80.

Cytochrome *c* oxidase from *P. denitrificans* was a kind gift from Dr. Bernd Ludwig, University of Lübeck, Lübeck, GFR. The enzyme contained 34.3 mol of heme *a*/mg of protein. Its concentration was determined as described (Ludwig & Schatz, 1979).

[2] The term "proton pump mechanism" is not used since cytochrome *c* oxidase cannot pump protons when not incorporated into closed membrane vesicles. The conformational transition is, however, thought to be a general property of the enzyme whether or not it leads to vectorial proton translocation.

Cytochrome *c* from horse heart and that from *Candida krusei* were type VI and type VII, respectively, from Sigma. Their concentration was determined from the isosbestic absorption at 410 nm (Margoliash & Frohwirt, 1959). Cytochrome *c* was reduced with an excess of sodium dithionite; excess reductant was removed on a small column (0.5 × 2 cm) of Sephadex G-25, which was eluted by spinning in a tabletop centrifuge (Bresnick, 1982).

Gel Permeation Chromatography. Sephacryl S-300 (Pharmacia) columns were run at 4 °C and calibrated with the following proteins (molecular weight, partition coefficient): thyroglobulin (669 000, 0.10), ferritin (440 000, 0.22), alcohol dehydrogenase (141 000, 0.43), bovine serum albumin (68 000, 0.57), chymotrypsinogen (25 000, 0.82), and cytochrome *c* (12 500, 0.96). A partition coefficient of zero corresponded to an apparent molecular weight of more than 2 000 000.

Analytical Ultracentrifugation. Sedimentation equilibrium runs were performed with a Beckman L5-75B centrifuge, equipped with a UV scanner, in a AN-G rotor at 4 °C. The protein was monitored at 278 nm. The protein distribution was analyzed by plotting the natural logarithm of the absorption at 278 nm versus the square of the radial displacement. The contribution of protein and detergent to the equilibrium distribution of the protein–detergent complex was resolved according to Reynolds and Tanford (1976), using H_2O and D_2O as solvents and a value of 1.22 g·cm^{-3} for the density of lauryl maltoside (Suarez et al., 1984). The molecular masses of the detergent and oxidase solutions in D_2O were corrected for proton–deuterium exchange (Edelstein & Schachman, 1967) by using correction factors in D_2O of k = 1.0155 for the protein and k = 1.0137 for lauryl maltoside (Suarez et al., 1984).

Photometric Titrations. Titration of cytochrome *c* oxidase solutions with cytochrome *c* was performed as before (Michel & Bosshard, 1984) except that the titration procedure was automated and that a mathematical correction for stray light was used (Michel, 1988a). Briefly, the precision syringe by which aliquots (10–50 μL) of the cytochrome *c* stock solution were added to the cytochrome *c* oxidase solution (2000 ± 0.2 μL) was driven by a computer-controlled stepper motor. Typically, the spectrum was measured in the range of 390–450 nm by a photodiode array spectrophotometer (Hewlett-Packard 8451). The instrument averaged over 50–100 individual spectra taken at 0.1-s intervals. Details of the experimental setup will be published elsewhere. The concentration of the cytochrome *c* oxidase was usually 4 μM, and cytochrome *c* was added in 20–40 aliquots until a ratio of heme *c*/heme aa_3 of 2.5 was reached. Measurements were performed at 25 °C. The total absorption after the last addition of cytochrome *c* was below 1.5 absorption units. The maximum absorption difference signal at 414 nm was 2% or less of the total absorption.

Kinetic Assays. The oxidation of reduced cytochrome *c* by cytochrome *c* oxidase was measured spectrophotometrically at 25 ± 0.1 °C in the range 548–552 nm for high substrate concentrations and in the range 418–420 nm for low substrate concentrations by using the Hewlett-Packard 8451 photodiode array spectrophotometer. Absorption differences were normalized to the absorption change at 580–586 nm, which was set to zero. The $\Delta\epsilon$ values used to calculate initial rates were 16.2 mM^{-1} cm^{-1} at 548–552 nm and 43.1 mM^{-1} cm^{-1} at 418–420 nm.

Assays were performed with a mixing robot. This device, which was built in our laboratory (Michel, 1988a,b), mixes variable amounts of substrate, enzyme, and buffer solution.

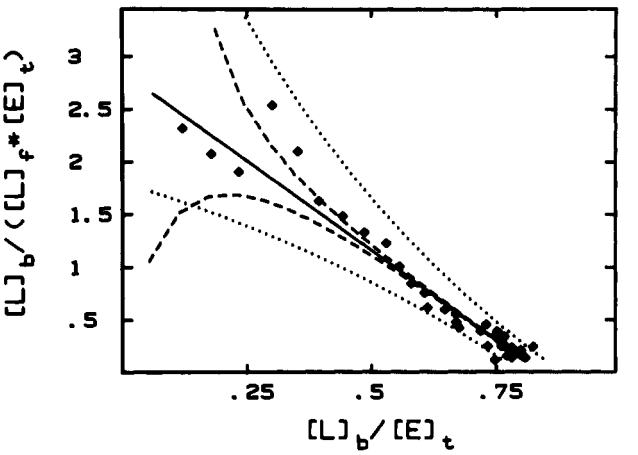

FIGURE 1: Error distribution in a Scatchard plot. The dotted line shows the error boundary for a ±5% error in $[L]_b/[E]_t$; the dashed line shows that for a ±1% error in $[E]_t$. L and E are ligand and enzyme, respectively. The subscripts b, f, and t indicate bound, free, and total, respectively. The experimental points are from a titration of dimeric oxidase with cytochrome *c*.

The assay mixture is transferred with a dead time of 0.2 s to a 1-cm flow cell placed in the HP 8451 spectrophotometer. The change of absorption is measured simultaneously at the two wavelength ranges specified above. The derivative of absorption versus time is calculated, and the rate is averaged over a time period adjusted to the rate of the reaction. The derivative is checked for linearity and noise and stored if the specified requirements are fulfilled.

For a single set of K_m and TN_{max} values three to four assays at 20 different concentrations of cytochrome *c*, ranging from 0.15 to 30 μM, were performed. This amounts to 60–80 single assays. The K_m and TN_{max} values of Tables III and IV are averages of several determinations totaling several hundred individual rate assays. The reproducibility of the assay procedure was superior to that of a manual initial rate assay.

Analysis of Primary Data. Unbiased data analysis was of prime importance to distinguish between linear and nonlinear binding and steady-state kinetics. Traditionally, the primary data are transformed and graphically represented by a linearized equation, typically a Scatchard plot for binding data and the corresponding Eadie–Hofstee plot for kinetic data. The inherent drawback of data analysis by a Scatchard or Eadie–Hofstee plot is not appreciated widely enough. First, the error grows exponentially at low concentrations of free ligand or total substrate (Figure 1). Second, an error in a relational parameter, such as in the case of the photometric titration, may artificially lead to a nonlinear plot for binding of a ligand to a single binding site. Therefore, the primary binding and titration data were not analyzed by a conventional linearization procedure. A numerical analysis of the primary data was employed instead. The binding data were fit to the equations

$$\frac{[C]_b}{[E]_t} = \frac{K[C]}{1 + K[C]} \quad (1)$$

$$\frac{[C]_b}{[E]_t} = \frac{K_1[C] + 2K_1K_2[C]^2}{1 + K_1[C] + K_1K_2[C]^2} \quad (2)$$

$[C]_b$ and $[C]$ are the concentrations of bound and free cytochrome *c*, respectively; $[E]_t$ is the total enzyme concentration; and K, K_1, and K_2 are the stoichiometric binding constants (Klotz & Hunston, 1979). The total enzyme concentration is

$$[E]_t = n[aa_3]_t \quad (3)$$

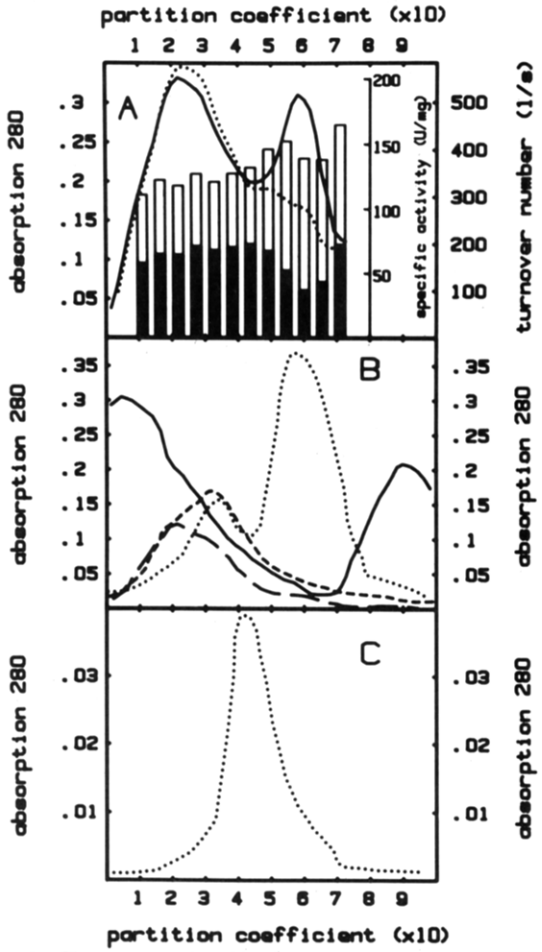

FIGURE 2: Chromatography of beef heart oxidase on Sephacryl S-300. (A) Oxidase (160 nmol of heme aa_3) in 0.1% lauryl maltoside, 10 mM Tris-HCl, pH 7.8, and 100 mM KCl was eluted on a Sephacryl S-300 column (2.4 × 80 cm) equilibrated in the same buffer. The eluate was monitored for absorption at 280 (—) and 420 nm (···, left ordinate divided by 2.5). Twelve pools were made and analyzed for enzyme activity (open bars) and specific activity (closed bars). (B) Rechromatography of pool 3 (– –), pool 6 (- - -), and pool 9 (···) from the chromatography shown in (A) (numbering of pools from the left) on a Sephacryl S-300 column (0.9 × 60 cm). Buffer as in (A). Elution of oxidase in 0.2% Tween 80, 10 mM Tris-HCl, pH 7.8, and 100 mM KCl on the same column (—). (C) Chromatography of monomeric (Triton X-100 treated) oxidase on Sephacryl S-300. Conditions as in (B).

where $[aa_3]_t$ is the total concentration of heme aa_3, measured photometrically, and n is the number of binding sites per heme aa_3. The concentration of bound cytochrome c is given by

$$\Delta A = \Delta\epsilon[C]_b \tag{4}$$

where ΔA is the measured absorption difference.

ΔA obtained at different ratios of heme c/heme aa_3 was fitted through relationships 3 and 4 to eq 1 and 2 by using a grid and gradient search routine (Michel, 1988a). $\Delta\epsilon$ and n were kept floating during the fitting procedure; hence $\Delta\epsilon$ and n were not biased by a priori assumptions. The fitting procedure used a weighted least-squares grid and gradient search program. The weight of each data point was taken as the inverse variance of the experimental signal obtained from several independent measurements. The decision for a one-site or a two-site model was based on the comparison of the root of least squares of fits to eq 1 and 2, respectively. The decision was made in favor of the simpler model if the root mean squares of the best fit to eq 1 were less than 30% larger than the root mean squares of the best fit to eq 2.

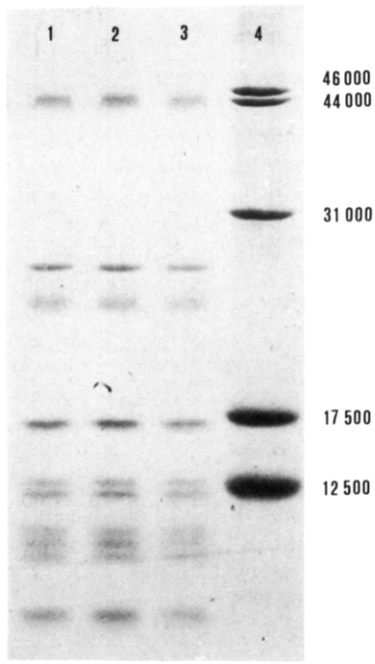

FIGURE 3: Polypeptide composition of cytochrome *c* oxidase eluted from Sephacryl S-300 determined by polyacrylamide gel electrophoresis in the presence of SDS (15% gel; Laemmli, 1970). Lane 1, cytochrome *c* oxidase from pool 3 of Figure 2A; lane 2, pool of Figure 2A; lane 3, pool 9 of Figure 2A; lane 4, molecular weight markers for aspartate aminotransferase (46 000 and 44 000), carboanhydrase (31 000), lysozyme (17 500), and cytochrome *c* (12 500).

The primary data from the kinetic measurements were fit to the equations

$$\frac{1}{[aa_3]_t}\frac{d[C]_t}{dt} = \frac{TN_{max}[C]_t}{K_m + [C]_t} \tag{5}$$

$$\frac{1}{[aa_3]_t}\frac{d[C]_t}{dt} = \frac{TN_{max1}[C]_t}{K_{m1} + [C]_t} + \frac{TN_{max2}[C]_t}{K_{m2} + [C]_t} \tag{6}$$

by the same fitting routine used for the photometric titration. TN_{max} and K_m values were floating parameters, and $[aa_3]_t$ was determined photometrically. The decision between a linear and a nonlinear kinetic model was made by comparing the root mean squares of the best fits to eq 5 and 6.

Results

Aggregation State of Cytochrome c Oxidase. A careful characterization of the aggregation state of the oxidase was crucial to test the kinetic mechanisms. Gel filtration was reported to separate different aggregates of the enzyme (Rosevear et al., 1980; Nalecz et al., 1986). Beef heart oxidase, isolated according to the method of Hartzell and Beinert (1974), was chromatographed on a column of Sephacryl S-300 (Figure 2A). The enzyme eluted as a mixture of different aggregation states, as was revealed by sedimentation equilibrium analysis of individual fractions. None of the 12 fractions of Figure 2A analyzed by analytical ultracentrifugation displayed a linear plot of ln A_{278} versus r^2, the square of the radial displacement. The inhomogeneity was more pronounced after 48 h of centrifugation, indicating a slow equilibrium between different aggregation states. In support of this, rechromatography of pools from the first Sephacryl column revealed a marked heterogeneity (Figure 2B).

All of the enzyme eluted from the Sephacryl column had the same polypeptide composition (Figure 3). In particular, the enzyme eluting with an apparent molecular mass of 100 kDa or less (partition coefficient around 0.6 in Figure 2A) had

the same polypeptide composition, totaling to about 200 kDa, as had the large enzyme aggregates appearing with the void volume of the Sephacryl column. We believe this material was partially adsorbed to the gel matrix and was eluted by the detergent-containing buffer in a reversed-phase manner. In support we found that most of the enzyme eluted as 100-kDa material when KCl was omitted from the elution buffer (not shown). Protein adsorption to the gel matrix is known to be highest at low ionic strength. The reported separation of oxidase into monomers by gel chromatography at low ionic strength must therefore be interpreted with caution (Nalecz et al., 1983; Bolli et al., 1985). If there was any monomeric oxidase at all in the eluate shown in Figure 2A, it was only partially separated from the dimeric material because the hydrodynamic radii of monomers and dimers differ by only 20% (Robinson & Talbert, 1986).

In 0.2% Tween 80 about 50% of the enzyme eluted at the void volume of the Sephacryl column with a molecular mass of 800 kDa or more (Figure 2B). The enzyme dispersed in Tween 80 was therefore regarded as "oligomeric". Lauryl maltoside efficiently diminished the amount of oligomeric enzyme (compare the solid line of Figure 2, panels A and B). In no case, however, was it possible to get uniformly dimeric enzyme by gel filtration. The oxidase dispersed in 0.2% lauryl maltoside was nevertheless regarded as "dimeric" since dimers constituted a major aggregation state in this detergent (Figure 2A).

Georgevich et al. (1983) reported the preparation of stable monomeric oxidase by treatment with high concentrations of Triton X-100 at slightly elevated pH. During this treatment some of the polypeptide subunit III was lost. Monomeric oxidase prepared in this way was brought into the lauryl maltoside–Tris buffer used for binding and kinetic experiments and chromatographed on the calibrated Sephacryl column. The material eluted with an apparent mass of 350 kDa (Figure 2C). The sedimentation equilibrium distribution was recorded in H_2O and D_2O. Plots of ln A_{280} versus r^2 were only slightly nonlinear after sedimentation times of 14 and 38 h. The nonlinearity was due to contaminating UV-absorbing impurities in the detergent micelles. Extrapolation of the apparent molecular mass of the Triton X-100 treated oxidase to the density of lauryl maltoside and correction for exchanged protons resulted in effective molecular masses of 200 ± 20 kDa for the protein, 117 ± 10 kDa for the detergent micelle, and 320 ± 20 kDa for the protein–detergent complex. The molecular mass was independent of the initial concentration of the protein (2.7–45 μM) and in excellent agreement with the molecular mass of 203 kDa for the sum of the 13 subunits (Buse et al., 1985). The Triton X-100 treated material was used as monomeric beef heart oxidase in subsequent experiments.

Photometric Binding Titration. Binding of cytochrome *c* to cytochrome *c* oxidase perturbs the optical absorption spectrum of cytochrome *c* in the α-, β-, and γ-bands of ferric and ferrous heme *c* (Michel & Bosshard, 1984). The spectral change at saturation of the oxidase with cytochrome *c* is of the order of $\Delta\epsilon$ = 5–10 mM^{-1} cm^{-1}, depending on ionic strength and detergent conditions (Tables I and II). The absorption difference signal at different ratios of heme *c*/heme aa_3 was fitted to eq 1 and 2, which describe a one-site and a two-site binding model, respectively. In comparing binding models, a numerical fit of the primary titration data to different binding equations is superior to a fit of the transformed binding data to the Scatchard equation, because the $\Delta\epsilon$ used to calculate the concentration of bound cytochrome *c* and the number *n* of binding sites per heme aa_3 are floating parameters in the numerical fitting procedure (see Experimental Procedures).

Table I: Comparison of Fits to One-Site and Two-Site Binding Models for the Binding of Cytochrome *c* to the Dimeric Beef Enzyme[a]

model	μ (mM)	K_1 (μM)	K_2 (μM)	$\Delta\epsilon_{414}$ (mM^{-1} cm^{-1})	n^b	noise[c]
one site[d]	24	0.07		6.15	0.7	0.12
	49	0.29		5.03	0.84	0.10
	74	1.63		6.57	1.2	0.12
two site[e]	24	0.03	0.15	5.85	0.68	0.10
	49	0.31	0.77	5.14	0.74	0.11
	74	2.31	3.88	6.85	0.53	0.14

[a] Photometric titrations were performed in 10 mM Tris-HCl, pH 7.4, and 0.1% lauryl maltoside and at the ionic strength (μ) indicated. [b] Number of binding sites per heme aa_3. [c] Root mean squares of best fit. [d] Fit to eq 1. [e] Fit to eq 2.

Table II: Photometric Titration of Oligomeric and Monomeric Beef Oxidase and Monomeric *P. dentrificans* Oxidase by Cytochrome *c*[a]

oxidase	μ (mM)	TN_{max1} (s^{-1})	K_{m1} (μM)	TN_{max2} (s^{-1})	K_{m2} (μM)
oligomeric beef[d]	24	0.23	10.2	0.78	0.13
	49	0.59	7.9	0.89	0.10
monomeric beef[e]	24	0.11	6.2	0.72	0.15
	49	1.27	8.1	0.75	0.09
P. denitrificans[e]	24	0.86	6.77	1.00	0.18
	49	0.97	3.35	0.86	0.10

[a] Values obtained from best fit to eq 1. [b,c] See Table I. [d] 10 mM Tris-HCl, pH 7.4, and 0.2% Tween 80. [e] As footnote *d* but with 0.1% lauryl maltoside.

The decision between a one-site model and a two-site model was made by comparing the root mean squares of the best fits to eq 1 and 2. This comparison is inherently difficult because there is no general rule for the comparison of fits to models with different degrees of freedom, as represented by the one-site and the two-site models, the latter having a lower degree of freedom. The model with the higher degree of freedom, i.e., the simpler model, must be favored if the root mean squares of the best fits are similar.

Table I shows the results for the dimeric beef heart oxidase at different ionic strength. The root mean squares are small and similar for the one-site and the two-site models. Hence, there can be no cooperativity between the binding sites for cytochrome *c* on dimeric oxidase. There is a single cytochrome *c* binding site per heme aa_3, in contradiction to the regulatory site mechanism.

The values of K_1 and K_2 from the best fit to the two-site model provide another argument against cooperativity between binding sites. In an enzyme with negative cooperativity between two binding sites, the ratio of the stoichiometric binding constants, K_2/K_1, is greater than 4 (Klotz & Hunston, 1979). Ratios of 5.00, 2.48, and 1.68 are obtained from best fits at 24, 49, and 74 mM ionic strength (Table I). These ratios make little sense; they indicate negative cooperativity at 24 mM and positive cooperativity at higher ionic strength.

Photometric titration of oligomeric and monomeric beef oxidase and of monomeric oxidase from *P. denitrificans* was also linear. The dissociation constants for the single site per heme aa_3 are compiled in Table II. Figure 4 shows the difference absorption spectra for different complexes and the Scatchard plots for dimeric and monomeric oxidase. The Scatchard plots were obtained from the titration data by using $\Delta\epsilon$, *n*, and *K* obtained by the numerical analysis. The plots

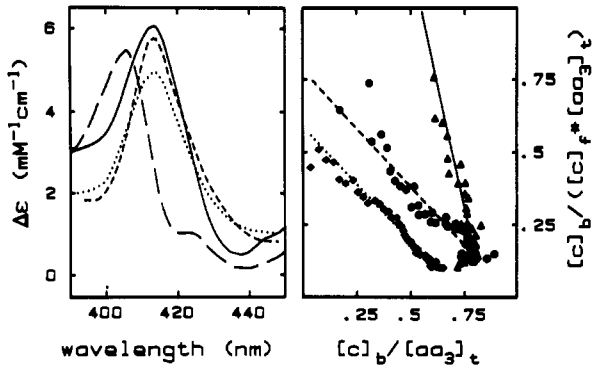

FIGURE 4: Photometric binding titration. (A) Difference spectra for 1:1 cytochrome *c* oxidase–cytochrome *c* complexes (spectrum of complex minus sum of components). Oligomeric beef oxidase in 0.2% Tween 80 (—); dimeric beef oxidase in 0.1% lauryl maltoside (- - -); monomeric beef oxidase in 0.1% lauryl maltoside (···); *P. denitrificans* oxidase (– –). Buffer: 10 mM Tris-HCl, pH 7.4, and 40 mM NaCl, μ = 49 mM. (B) Scatchard transformation of the photometric titration data for dimeric beef oxidase (▲), monomeric beef oxidase (◆), and *P. denitrificans* oxidase (●).

Table III: Kinetic Parameters for the Oxidation of Cytochrome *c* by Dimeric and Monomeric Beef Oxidase and by Oxidase from *P. denitrificans*[a]

oxidase	μ (mM)	TN_{max1} (s^{-1})	K_{m1} (μM)	TN_{max2} (s^{-1})	K_{m2} (μM)	noise[b]
dimeric beef	24	77	0.73	9.5	33	0.22
	49	49	0.54	29	5.74	0.56
	74	56	1.51	35	7.8	0.81
	99	47	1.60	36	18.6	0.80
	150	69	6.6			1.06
monomeric beef	24	39	1.0	10	21	0.37
	49	30	0.3	26	5.3	0.56
	74	44	0.8	39	5.6	0.70
	99	55	0.9	23	7	0.76
P. denitrificans	24	34	0.2	92	15	1.17
	49	45	1.8	85	11	0.65
	74	92	14			0.32
	99	96	35			0.38

[a] 10 mM Tris-HCl, pH 7.4, and 0.1% lauryl maltoside; ionic strength adjusted with NaCl. [b] Root mean squares of best fit to eq 6.

are not transformations of the titration data using a predetermined $\Delta\epsilon$, as in a conventional Scatchard-type analysis.

Kinetics of Cytochrome c Oxidation. The photometric assay was used to measure the rate of cytochrome *c* oxidation. Assays were performed by an automatic procedure based on a mixing robot connected to a photodiode array spectrophotometer. Initial rates were fitted to eq 5 and 6 and the root mean squares of the best fits were compared to decide between biphasic and monophasic reactions. Table III summarizes the kinetic parameters for the dimeric and monomeric oxidase. The values were obtained at 24–150 mM ionic strength in 10 mM Tris-HCl, pH 7.4, and 0.1% lauryl maltoside. The kinetics were biphasic up to about 100 mM ionic strength and monophasic at higher ionic strength. With the *P. denitrificans* oxidase the reaction was monophasic above 50 mM ionic strength. Essentially the same results were obtained when the enzyme was dispersed in 0.2% Tween 80 or 0.2% Triton X-100, except that TN_{max} values were lower in Tween and much lower in Triton (data not shown), as reported previously (van Buuren & van Gelder, 1974; Robinson & Capaldi, 1977; Sinjorgo et al., 1987). The observation of biphasic kinetics with monomeric oxidase from beef and *P. denitrificans* contradicts the negative cooperativity model.

Table IV shows the kinetic parameters for dimeric and monomeric oxidase at pH values from 5.6 to 8.6 and 49 mM ionic strength. Interestingly, the reaction is monophasic at lower pH values. The different buffer salts used at low and high pH, Tris and Bistris, had no influence on the values of K_m and TN_{max}. The TN_{max} values increased considerably with decreasing pH to reach rates in excess of 300 s^{-1} at pH 5.6 for the dimeric enzyme. There is no pH optimum for the maximum turnover number within the pH range 5.6–8.6. The same observation was reported by Sinjorgo et al. (1986). K_m values increase at lower pH.

Table IV: pH Dependence of the Oxidation of Cytochrome *c* by Dimeric and Monomeric Oxidase

oxidase	pH[a]	TN_{max1} (s^{-1})	K_{m1} (μM)	TN_{max2} (s^{-1})	K_{m2} (μM)	noise[b]
dimeric beef	8.6	30	0.4	21	16	0.93
	8.0	59	0.5	52	2.4	2.4
	7.4	122	0.7	70	4.4	2.7
	6.8	265	1.6	0		3.3
	6.2	334	1.9	0		7.4
	5.6	344	2.4	0		3.4
monomeric beef	8.6	7.4	0.6	22	9	0.2
	8.0	17	0.5	32	11	1.0
	7.4	77	2.0	64	67	1.1
	6.8	188	2.6	0		4.6
	6.2	259	3.1	0		5.4
	5.6	258	2.8	0		4.9
P. denitrificans	8.6	15	0.8	11	16	0.4
	8.0	35	1.7	44	16	1.3
	7.4	14	1.8	132	5.4	2.1
	6.8	187	2.6			3.5
	6.2	238	7.9			3.1
	5.6	270	9.9			2.0

[a] 10 mM Tris-HCl at pH 7.4, 8.0, and 8.6; 10 mM [bis(2-hydroxyethyl)amino]tris(hydroxymethyl)methane hydrochloride (Bistris) at pH 7.4, 6.8, 6.2, and 5.6. Buffers contained in addition 0.1% lauryl maltoside and sufficient NaCl to reach μ = 49 mM. [b] Root least squares of best fit to eq 6 (biphasic reaction) or 5 (monophasic reaction).

Examples of Eadie–Hofstee transformations of the rate of cytochrome *c* oxidation are shown in Figure 5A–C. The Eadie–Hofstee plots of Figure 5 are based on the kinetic parameters obtained by fits to eq 5 and 6. In other words, the decision about linearity or nonlinearity of the reaction was not based on the inspection of a Eadie–Hofstee plot constructed from initial rate data.

Dissociation constants and K_{m1} values differed by factors of 2–10, and the K_{m1} value was the higher of the two. The same observation was made with oligomeric beef oxidase reacting with horse and *C. krusei* cytochrome *c*. The values obtained with *C. krusei* cytochrome *c* were K_{m1} = 1.24 μM, K_{m2} = 38.8 μM, and K = 0.07 μM. For horse cytochrome *c* the corresponding values measured under the same conditions were K_{m1} = 0.43 μM, K_{m2} = 27 μM, and K = 0.15 μM. Thus, there is no apparent correlation between K_m values and dissociation constants except that the latter is always significantly smaller. Previously, similar or identical values for the dissociation constant of the oxidase–cytochrome *c* complex (obtained by equilibrium gel filtration) and the K_m of the high-affinity/low-velocity reaction phase have been reported (Ferguson-Miller et al., 1976, 1978; Staudenmeyer et al., 1976; Osheroff et al., 1980), in support of rate-limiting product dissociation (Speck et al., 1984; Sinjorgo et al., 1986). We therefore tried to fit the initial rate data to eq 6 while keeping K_{m1} fixed at the values of K obtained from the photometric titration (Tables I and II). The fits were very poor.

Our results are compatible with the predictions of the conformational transition mechanism: biphasic kinetics with both monomeric and dimeric oxidase and linear binding curves in the absence of electron transfer. Since the conformational

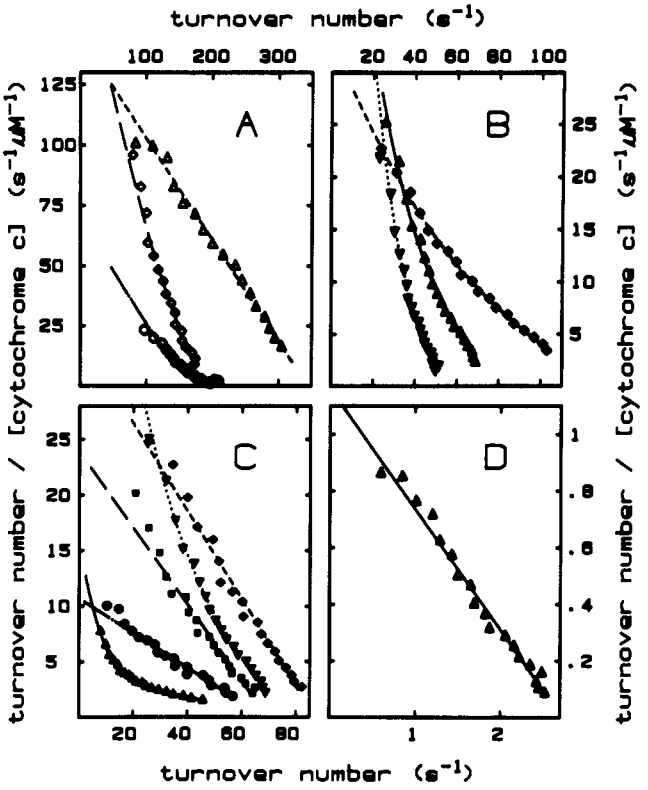

FIGURE 5: Eadie–Hofstee transformation of the steady-state rate of cytochrome *c* oxidation. (A) Dimeric beef oxidase at pH 5.6 (△), 7.4 (◇), and 8.6 (○). For the pH 8.6 curve the abscissa must be divided by 6. Conditions as in Table IV. (B) Dimeric beef oxidase (▲); monomeric beef oxidase (▼); oxidase from *P. denitrificans* (◆). Conditions as in Table III, μ = 49 mM. (C) Dimeric beef oxidase at ionic strength of 24 mM (▲), 49 mM (▼), 74 mM (◆), 99 mM (■), and 150 mM (●). Conditions as in Table III. (D) Beef oxidase treated with chymotrypsin (see Experimental Procedures). Conditions: 10 mM Tris-HCl, pH 7.4, 0.2% Tween 80, μ = 24 mM.

transition mechanism demands a tight coupling between electron transfer and proton pumping, we have attempted to decouple the two processes by brief proteolysis of the enzyme with chymotrypsin, in the hope that such treatment will partially destroy the structural integrity of the enzyme. Limited proteolysis was shown to remove subunit III and to interfere with the pumping of protons (Puettner et al., 1985). Remarkably, the chymotrypsin-treated oxidase showed monophasic kinetics (Figure 5D). The rate of cytochrome *c* oxidation was strongly decreased to TN_{max} = 2.7 s^{-1}, as compared to 111 s^{-1} for the intact dimeric enzyme in the same buffer. The single K_m was 2.35 μM, a value between the 0.2 and 15 μM obtained for K_{m1} and K_{m2}, respectively, of the intact enzyme.

Discussion

The steady-state oxidation of cytochrome *c* catalyzed by cytochrome *c* oxidase has been analyzed by many different investigators. Several of the data reported here are, in essence, a confirmation of earlier work by others (Ferguson-Miller et al., 1976; Sinjorgo et al., 1986). Our aim was to do a comprehensive comparison between the steady-state kinetic assay and the dissociation of the oxidase–cytochrome *c* complex. As has been outlined in the introduction, such a comparison is of help in evaluating the three currently discussed mechanisms for cytochrome *c* oxidation.

The present data agree with a conformational transition mechanism. They are not in agreement with the negative cooperativity mechanism. The contradiction with the regulatory site mechanism is evident but less strict, as will be discussed shortly.

The aggregation state of detergent-solubilized oxidase is controversial, and the preparation of uniformly monomeric oxidase is difficult. We were unable to reproduce the low ionic strength separation of monomeric from dimeric beef oxidase (Nalecz et al., 1983, 1986) and had to resort to the more drastic monomerization procedure using high concentrations of Triton X-100 at slightly alkaline pH (Georgevich et al., 1983). This procedure removes some of subunit III. The physical mass of our monomeric oxidase was carefully checked by analytical ultracentrifugation and was consistent with the sum of masses of a single set of 12–13 subunits.

Binding of cytochrome *c* to cytochrome *c* oxidase has been measured by equilibrium gel filtration (Ferguson-Miller et al., 1976; Osheroff et al., 1980). By this technique binding of any sort is detected, provided that the association is stable enough under the gel filtration conditions. The reported binding isotherms were often nonlinear, indicating several types of binding sites or interaction between binding sites, or both. Cytochrome *c* has a net positive charge of 7–8 at neutral pH. It binds strongly to negative surfaces, for example, to phospholipid head groups of membranes (Nicholls, 1974). Stoichiometries above one heme *c* per heme aa_3 may be explained by this type of nonspecific binding.

The photometric titration method detects a small conformational perturbation in the area of the exposed heme edge (Weber et al., 1987), which is the area recognized by the catalytic site of cytochrome *c* oxidase [review by Margoliash and Bosshard (1983)]. Thus, the photometric method selects the "productively" bound cytochrome *c* molecules. The perturbation spectrum shown in Figure 4 is specific for the type of oxidase used. It cannot be mimicked by poly(glutamic acid), by small amounts of different alcohols, or by a change of ionic strength.[3]

Because the spectroscopic binding signal is very specific, one might argue that the binding of cytochrome *c* to a second, different site, as predicted in the regulatory site mechanism, goes undetected. Nevertheless, binding to a regulatory site would have been detected from the stoichiometry of the titration curve.[4] However, if binding at the regulatory site were very much weaker than at the catalytic site, it would go undetected. In the present case, the dissociation constant at the regulatory site would have to be above ~20 μM to make cooperativity between sites undetectable in the photometric titration experiment. Hence, the regulatory site model is not definitely ruled out by the results from the binding titration experiments. However, there is another contradiction to the regulatory site mechanism. The mechanism predicts equal or similar K_m values and dissociation constants. The present data are not in support of such an equality, with the proviso that our *K* values are not true dissociation constants for the binding of ferrous cytochrome *c* to "working" oxidase.

Binding to monomeric beef and *Paracoccus* oxidase was linear. In contrast, the kinetics were biphasic at low ionic strength and neutral pH. This finding is in direct contradiction to the negative cooperativity mechanism. In support of the negative cooperativity mechanism, monophasic kinetics was reported for the *Paracoccus* oxidase (Nalecz et al., 1985; Bolli et al., 1986), for subunit III depleted beef oxidase [Nalecz et

[3] Bruno Michel, unpublished observation.

[4] The signal of the photometric titration is a function of the total amount of cytochrome *c* added per heme aa_3. The signal would saturate at two hemes *c* per heme aa_3 if there were two binding sites, even if the second site were photometrically silent.

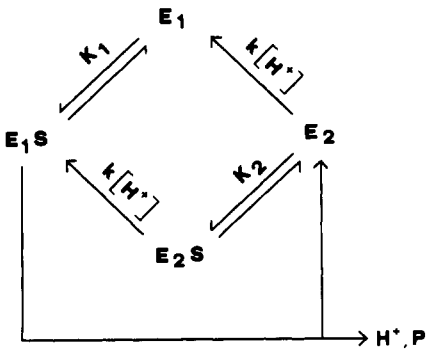

FIGURE 6: A minimal scheme for a conformational transition mechanism. E_1 and E_2 indicate cytochrome *c* oxidase in different conformational states; S and P are the substrate (ferrous cytochrome *c*) and the product (ferric cytochrome *c*); K_1 and K_2 are the dissociation constants of substrate binding to E_1 and E_2, respectively; k is the second-order rate constant for the pH-dependent conformational transition. See text for details.

al., 1985; see however Suarez et al. (1984) and Prochaska and Reynolds (1986)], and for monomeric beef oxidase prepared by dissociation at low ionic strength [Bolli et al., 1985; see however Hakvoort et al. (1988)]. The discrepancy with our data might be due to the larger number of experimental data points in our experiments, to the increased accuracy of the automatic assay procedure, or to our careful numerical analysis of the primary rate data. Previously, monophasic kinetics were deduced from Eadie–Hofstee plots that were based on a smaller number of experimental points (Bolli et al., 1985, 1986; Nalecz et al., 1985).

We ourselves fell victim to the conventional linerization procedure in our previous report on the photometric titration of cytochrome *c* oxidase with cytochrome *c* (Michel & Boshard, 1984). There, the nonlinear Scatchard plots were the result of fitting of the titration data to eq 2 while keeping $\Delta\epsilon$ and n fixed. Applying the improved fitting procedure to the former data, one obtains linear binding curves.[3]

The conformational transition mechanism, with which the present data are in agreement, was formulated to explain the well-established proton-pumping property of the oxidase. The mechanism of Brzezinski and Malmström, which accounts for biphasic kinetics in the context of a proton pump, does not explain why at low pH the steady-state rate increases and becomes monophasic (Brzezinski & Malmström, 1986, 1987; Brzezinski et al., 1986). We propose a minimal mechanism which explains the rate increase at decreasing pH as well as the fact that K_{m1} is larger than the substrate dissociation constant K_1 (Figure 6). The enzyme exists in two different conformations, E_1 and E_2. Binding of cytochrome *c* to E_2 is weaker than to E_1 ($K_1 < K_2$ in Figure 6). E_1 is the form of the enzyme that takes up the proton(s) (the controversial H^+/e^- stoichiometry is irrelevant in the present discussion). E_2 is the form of the enzyme after the release of the proton(s). When the uptake and release of protons are tightly coupled to the electron-transfer reaction, the transitions from E_1 to E_2 and back to E_1 are unidirectional, as indicated. The redox state of E_1 and E_2 is unimportant in the context of the present discussion. It may conform to some mixed-state characteristic of "working" oxidase. The loop connecting E_1S with E_2 encompasses several steps: the oxidation of a single molecule of cytochrome *c* in the simplest case, but more probably the oxidation of two substrate molecules since a two-electron reduction is required for rapid internal electron transfer between the redox centers of cytochrome *c* oxidase (Fabian et al., 1987). Most importantly, the release of one or several protons is mandatory in reaching E_2. Once in state E_2 the enzyme has two possibilities. Either E_2 reverts directly to E_1 and a new round of cytochrome *c* oxidation begins. This is the simple, monophasic Michaelis–Menten pathway of eq 5. Alternatively, E_2 binds a molecule of cytochrome *c* before the conformational transition and reverts to E_1 with the substrate already bound. Since $K_1 < K_2$, the latter pathway is only important at high concentrations of cytochrome *c*, and the kinetics become biphasic.

At high ionic strength K_1 increases and may coincide with K_2. The second-order rate constant for cytochrome *c* oxidation does indeed decrease at increasing ionic strenth (Veerman et al., 1983). Alternatively, both K_1 and K_2 increase at increasing ionic strength, and the reaction becomes "pseudo-monophasic" because the second phase is no longer detectable at the highest cytochrome *c* concentration tested (30 μM in the present case).

An increase of the proton concentration will speed up the direct conformational transition from E_2 to E_1. The direct transition will be much faster than the pathway $E_2 \rightarrow E_2S \rightarrow E_1S$, resulting in monophasic kinetics at low pH. Again the rate may be pseudo-monophasic because the second phase is no longer detected at the highest substrate concentration tested.

By the mechanism shown in Figure 6 we can also explain why the substrate dissociation constant is lower than K_{m1}: there is no rate-limiting product release in the mechanism of Figure 6. K_{m1} is composed of the dissociation constant K_1,[5] the rate constant for the loop between E_1S and E_2, and the pseudo-first-order rate constant $k[H^+]$. The latter increases with decreasing pH, giving rise to higher K_m values at lower pH, as observed here (Table IV) and by Sinjorgo et al. (1986).

As a test for the validity of the conformational transition mechanism, the linkage between electron transfer and proton pumping was destroyed and the kinetics of the altered enzyme analyzed. To this end, cytochrome *c* oxidase was briefly digested with chymotrypsin. Such limited proteolysis can inhibit proton pumping to variable degrees (Puettner et al., 1985). Indeed, the chymotrypsin-treated oxidase shows monophasic behavior. This observation conforms with the expectation that the conformational transition depends on the structural integrity of the enzyme.

ACKNOWLEDGMENTS

We are much indebted to Dr. Bernd Ludwig, University of Lübeck, Lübeck, GFR, for a sample of cytochrome *c* oxidase from *P. denitrificans*.

Registry No. Cytochrome *c* oxidase, 9001-16-5; cytochrome *c*, 9007-43-6.

REFERENCES

Antalis, T. M., & Palmer, G. (1982) *J. Biol. Chem. 257*, 6194–6206.

Bolli, R., Nalecz, K. A., & Azzi, A. (1985) *Arch. Biochem. Biophys. 240*, 102–116.

Bolli, R., Nalecz, K. A., & Azzi, A. (1986) *J. Bioenerg. Biomembr. 18*, 277–284.

Bradford, M. (1976) *Anal. Biochem. 72*, 248–254.

Bresnick, E. (1982) in *Cytochrome P-450 Monooxygenase Systems* (Schenckmann, J. B., & Kupfer, D., Eds.) p 191, Pergamon, New York.

Brzezinski, P., & Malmström, B. G. (1986) *Proc. Natl. Acad. Sci. U.S.A. 83*, 4282–4286.

Brzezinski, P., & Malmström, B. (1987) *Biochim. Biophys. Acta 894*, 29–38.

[5] The constant K_1 of Figure 6 may be close to the dissociation constant K obtained for binding of ferric cytochrome *c* to the resting, fully oxidized oxidase (Tables I and II).

Brzezinski, P., Thörnström, P. E., & Malmström, B. G. (1986) *FEBS Lett. 194*, 1–5.
Buse, G., Meinecke, L., & Bruch, B. (1985) *J. Inorg. Biochem. 23*, 149–153.
Capaldi, R. A., Darley-Usmar, V., Fuller, S., & Millett, F. (1982) *FEBS Lett. 138*, 1–7.
Chen, P. S., Toribara, T. Y., & Warner, H. (1956) *Anal. Chem. 28*, 1756–1758.
Darley-Usmar, V. M., Georgevich, G., & Capaldi, R. A. (1983) *FEBS Lett. 166*, 131–135.
Edelstein, S. J., & Schachman, H. K. (1967) *J. Biol. Chem. 242*, 306–311.
Errede, B., Haight, G. P., Jr., & Kamen, M. D. (1976) *Proc. Natl. Acad. Sci. U.S.A. 73*, 113–117.
Fabian, M., Thornström, P. E., Brzezinsky, P., & Malmström, B. G. (1987) *FEBS Lett. 213*, 396–400.
Ferguson-Miller, S., Brautigan, D. L., & Margoliash, E. (1976) *J. Biol. Chem. 251*, 1104–1115.
Ferguson-Miller, S., Brautigan, D. L., & Margoliash, E. (1978) *J. Biol. Chem. 253*, 149–159.
Fuller, S. D., Capaldi, R. A., & Henderson, R. (1979) *J. Mol. Biol. 134*, 305–327.
Georgevich, G., Darley-Usmar, V. M., Malatesta, F., & Capaldi, R. A. (1983) *Biochemistry 22*, 1317–1322.
Hakvoort, T. B. M., Moolenaar, K., Lankvelt, A. H. M., Sinjorgo, K. M. C., Dekker, H. L., & Muijsers, A. O. (1988) *Biochim. Biophys. Acta 894*, 347–354.
Hartzell, C. R., & Beinert, H. (1974) *Biochim. Biophys. Acta 368*, 318–338.
Keilin, D. (1930) *Proc. R. Soc. London, B 106*, 418–444.
Klotz, I. M., & Hunston, D. L. (1979) *Arch. Biochem. Biophys. 193*, 314–328.
Laemmli, U. K. (1970) *Nature (London) 227*, 680–685.
Ludwig, B. (1980) *Biochim. Biophys. Acta 594*, 177–189.
Ludwigh, B., & Schatz, G. (1979) *Proc. Natl. Acad. Sci. U.S.A. 77*, 196–200.
Ludwig, B., Grabo, M., Gregor, I., Lustig, A., Regenass, M., & Rosenbusch, J. (1982) *J. Biol. Chem. 257*, 5576–5578.
Malmström, B. G. (1985) *Biochim. Biophys. Acta 811*, 1–12.
Margoliash, E., & Frohwirt, N. (1959) *Biochem. J. 71*, 570–572.
Margoliash, E., & Bosshard, H. R. (1983) *Trends Biochem. Sci. (Pers. Ed.) 8*, 316–320.
Michel, B. (1988a) Ph.D. Dissertation, University of Zurich, Faculty of Science.
Michel, B. (1988b) Swiss Patent Pending 321/88-4.
Michel, B., & Bosshard, H. R. (1984) *J. Biol. Chem. 259*, 10085–10091.
Minnaert, K. (1961) *Biochim. Biophys. Acta 50*, 23–34.
Nalecz, K. A., Bolli, R., & Azzi, A. (1983) *Biochem. Biophys. Res. Commun. 114*, 822–828.
Nalecz, K. A., Bolli, R., Ludwig, B., & Azzi, A. (1985) *Biochim. Biophys. Acta 808*, 259–272.
Nalecz, K., Bolli, R., & Azzi, A. (1986) *Methods Enzymol. 126*, 45–64.
Nicholls, P. (1965) in *Oxidases and Related Redox Systems* (King, T. E., Mason, H. S., & Morrison, M., Eds.) pp 764–777, Wiley, New York.
Nicholls, P. (1974) *Biochim. Biophys. Acta 346*, 261–310.
Nicholls, P., & Chance, B. (1974) in *Molecular Mechanisms of Oxygen Activation* (Hayaishi, O., Ed.) pp 479–534, Academic, New York.
Osheroff, N., Brautigan, D. L., & Margoliash, E. (1980) *J. Biol. Chem. 255*, 8245–8251.
Poole, R. K. (1983) *Biochim. Biophys. Acta 726*, 205–243.
Prochaska, L. J., & Reynolds, K. A. (1986) *Biochemistry 25*, 781–787.
Puettner, I., Carafoli, E., & Malatesta, F. (1985) *J. Biol. Chem. 260*, 3719–3723.
Reynolds, J. A., & Tanford, C. (1976) *Proc. Natl. Acad. Sci. U.S.A. 73*, 4467–4470.
Robinson, N. C., & Capaldi, R. A. (1977) *Biochemistry 16*, 375–381.
Robinson, N. C., & Talbert, L. (1986) *Biochemistry 25*, 2328–2335.
Rosevear, P., VanAken, T., Baxter, J., & Ferguson-Miller, S. (1980) *Biochemistry 19*, 4108–4115.
Sinjorgo, K. M. C., Meijling, I. H., & Muijsers, A. O. (1984) *Biochim. Biophys. Acta 767*, 48–56.
Sinjorgo, K. M. C., Steinebach, O. M., Dekker, M. L., & Muijsers, A. O. (1986) *Biochim. Biophys. Acta 850*, 108–115.
Sinjorgo, K. M. C., Durak, I., Dekker, H. L., Edel, C. M., Bieleman, A. H. L., Back, N. B. T., Hakvoort, T. B. M., & Muijsers, A. O. (1987) *Biochim. Biophys. Acta 893*, 241–250.
Smith, L., & Conrad, H. E. (1956) *Arch. Biochem. Biophys. 63*, 403–413.
Speck, S. H., Dye, D., & Margoliash, E. (1984) *Proc. Natl. Acad. Sci. U.S.A. 81*, 347–351.
Staudenmayer, N., Smith, M. B., Smith, H. T., Spies, F. K., Jr., & Millett, F. (1976) *Biochemistry 15*, 3198–3205.
Steffens, G. C. M., Biewald, R., & Buse, G. (1987) *Eur. J. Biochem. 164*, 295–300.
Suarez, M. D., Revzin, A., Narlock, R., Kempner, E. S., Thompson, D. A., & Ferguson-Miller, S. (1984) *J. Biol. Chem. 259*, 13791–13799.
Van Buuren, K. J. H., & van Gelder, B. F. (1974) *Biochim. Biophys. Acta 333*, 209–217.
Van Gelder, B. F. (1966) *Biochim. Biophys. Acta 118*, 36–46.
Veerman, E. C. I., Wilms, J., Dekker, H. L., Muijsers, A. O., van Buuren, K. J. H., & van Gelder, B. F. (1983) *J. Biol. Chem. 258*, 5739–5745.
Wainio, W. W. (1983) *Biol. Rev. Cambridge Philos. Soc. 58*, 131–156.
Weber, C., Michel, B., & Bosshard, H. R. (1987) *Proc. Natl. Acad. Sci. U.S.A. 84*, 6687–6691.
Wikström, M., Kraab, K., & Saraste, H. (1981) *Cytochrome Oxidase: A Synthesis*, Academic, London.